Energy loss of a heavy fermion in an anisotropic QED plasma

Paul Romatschke and Michael Strickland
Institut für Theoretische Physik, Technische Universität Wien,Wiedner Hauptstrasse 8-10, A-1040 Vienna, Austria
(Received 10 October 2003; published 11 March 2004)

We compute the leading-order collisional energy loss of a heavy fermion propagating in a QED plasma with an electron distribution function which is anisotropic in momentum space. We show that in the presence of such anisotropies there can be a significant directional dependence of the heavy fermion energy loss with the effect being large for highly relativistic velocities. We also repeat the analysis of the isotropic case more carefully and show that the final result depends on the intermediate scale used to separate hard and soft contributions to the energy loss. We then show that the canonical isotropic result is obtained in the weak-coupling limit. For intermediate coupling we use the residual scale dependence as a measure of our theoretical uncertainty. We also discuss complications which could arise due to the presence of unstable soft photonic modes and demonstrate that the calculation of the energy loss is safe.

DOI: 10.1103/PhysRevD.69.065005 PACS number(s): 11.15.Bt, 04.25.Nx, 11.10.Wx, 12.38.Mh

I. INTRODUCTION

An understanding of the production, propagation, and hadronization of heavy quarks in relativistic heavy ion collisions is important for predicting a number of experimental observables including the heavy-meson spectrum, the single lepton spectrum, and the dilepton spectrum. The first experimental results for the inclusive electron spectrum have been reported [1] in addition to the first measurements of J/ψ production at the BNL Relativistic Heavy Ion Collider (RHIC) [2]. The measurement of the inclusive electron spectrum allows for a determination of heavy quark energy loss since it is primarily due to the semileptonic decay of charm quarks. The heavy fermion energy loss comes into play since it is necessary in order to predict the heavy fermion energy at the decay point. It is therefore important to have a thorough theoretical understanding of heavy fermion energy loss for a proper comparison with the experimental results. In this paper we will show that in QED there is a modification of the leading-order (collisional) heavy fermion energy loss if there is a momentum-space anisotropy in the electron distribution function. The motivation for this work is to provide a testing ground for techniques that can be applied to QCD in order to make predictions of the directional dependence of the collisional energy loss of a heavy fermion propagating through an anisotropic quark-gluon plasma.

In the last few years a more or less standard picture of the early stages of a relativistic heavy ion collision has emerged. In its most simplified form there are three assumptions: (1) that the system is boost invariant along the beam direction, (2) that it is homogeneous in the directions perpendicular to the beam direction, and (3) that the physics at early times is dominated by gluons with momentum at a ''saturation'' scale Q_s which have occupation numbers of order $1/\alpha_s$. The first two assumptions are reasonable for describing the central rapidity region in relativistic heavy-ion collisions. The third assumption relies on the presence of gluonic ''saturation'' of the nuclear wave function at very small values of the Bjorken variable x [3]. In this regime one can determine the growth of the gluon distribution by requiring that the cross section for deep inelastic scattering at fixed Q^2 does not violate unitarity bounds. As a result the gluon distribution function saturates at a scale Q_s changing from $1/k_\perp^2 \to \log(Q_s^2/k_\perp^2)/\alpha_s$. Luckily, despite this saturation, due to the factor of $1/\alpha_s$ in the second scaling relation the occupation number of small-x gluonic modes in the nuclear wave function is still large enough to determine their distribution function analytically using classical nonlinear field theory [3]. In the weak-coupling limit the assumptions above have been used by Baier et al. in an attempt to systematically describe the early stages of quark-gluon plasma evolution in a framework called ''bottom-up'' thermalization [4].

The resulting picture which emerges from using these assumptions is one in which the initial gluonic distribution function is extremely anisotropic in momentum space having the form

$$f(\mathbf{p},\mathbf{x}) = F(p_\perp)\,\delta(p_z). \tag{1}$$

This is, of course, an idealization. In a more realistic scenario the delta function above would have a small but finite width which increases as a function of time, but despite this finite width, the distribution function would still be extremely anisotropic in momentum space during the early stages of the collision. In anisotropic systems it has been shown that the physics of the QED and QCD collective modes changes dramatically compared to the isotropic case and instabilities are present which can accelerate the thermalization and isotropization of the plasma [5–11]. In fact, the paper of Arnold, Lenaghan, and Moore points out that the presence of anisotropies in the early stages of QGP evolution requires modification of the bottom-up thermalization scenario [11].

In our previous paper [10] we derived a tensor basis for the photon/gluon self-energy and calculated the corresponding structure functions for an anisotropic system in which the distribution function is homogeneous and obtained from an isotropic distribution function by the rescaling of only one direction in momentum space

$$f(\mathbf{p},\mathbf{x}) = N(\xi) f_{\rm iso}(p\sqrt{1+\xi(\hat{\mathbf{p}}\cdot\hat{\mathbf{n}})^2}), \tag{2}$$

where $N(\xi)$ is a normalization constant, $\hat{\mathbf{p}}$ is the particle 3-velocity, the unit vector $\hat{\mathbf{n}}$ specifies the anisotropy direction, and $-1<\xi<\infty$. Note that the distribution function given by Eq. (1) is obtained in the limit $\xi\to\infty$ assuming that Eq. (2) is normalized in the same way as Eq. (1).

Using classical kinetic field theory we were then able to numerically determine the photon/gluon self-energy structure functions for this tensor basis in the entire complex energy plane for arbitrary ξ. In this paper we will use these structure functions to determine the leading-order (collisional) energy loss of a heavy fermion propagating through an anisotropic QED plasma. This calculation will allow us to determine the dependence of the collisional energy loss on the angle of propagation θ_n, the parton velocity v, the coupling constant e, and the temperature T. We will show that for large anisotropies and velocities the directional dependence of the heavy fermion energy loss is large and could therefore lead to a significant experimental effect. During the development we will also discuss some technical details related to the cutoff dependence of the isotropic and anisotropic results.

The organization of the paper is as follows. In Sec. II we review some of the notation and results from Ref. [10]. In Sec. III A we calculate the contribution to the energy loss coming from the exchange of soft photons with momenta on the order of eT. In Sec. III B we discuss complications which could arise due to the presence of unstable soft photonic modes and show that the soft energy loss calculation is safe. In Sec. III C we calculate the contribution to the energy loss coming from the exchange of hard photons with momenta on the order of T. In Sec. IV we combine the soft and hard contributions to obtain the final isotropic and anisotropic results. In Sec. V we list the limitations of the treatment presented here and provide a short description of how the result contained here can be extended to QCD.

II. SETUP

In this section we will review some of the findings from our previous paper [10] which we will use in the subsequent sections.

A. Tensor basis

For anisotropic systems with only one preferred direction we construct a basis for symmetric 3-tensors that depends on a fixed anisotropy 3-vector $\hat{n}^i$ with $\hat{\mathbf{n}}^2=1$. Note that here and in the remainder of the text vector quantities with hats indicate unit vectors. We first define the projection operator

$$A^{ij}=\delta^{ij}-k^ik^j/k^2, \tag{3}$$

and use it to construct $\tilde{n}^i=A^{ij}\hat{n}^j$ which obeys $\tilde{n}\cdot k=0$. With this we can construct the tensors

$$B^{ij}=k^ik^j/k^2 \tag{4}$$

$$C^{ij}=\tilde{n}^i\tilde{n}^j/\tilde{n}^2 \tag{5}$$

$$D^{ij}=k^i\tilde{n}^j+k^j\tilde{n}^i. \tag{6}$$

Any symmetric 3-tensor $\mathbf{T}$ can now be decomposed into the basis spanned by the four tensors $\mathbf{A},\mathbf{B},\mathbf{C}$, and $\mathbf{D}$,

$$\mathbf{T}=a\mathbf{A}+b\mathbf{B}+c\mathbf{C}+d\mathbf{D}. \tag{7}$$

B. Self-energy structure functions

Converting the result of Ref. [10] from QCD to QED the spacelike components of the high-temperature photon self-energy for particles with soft momentum ($k\sim eT$) can be written as

$$\Pi^{ij}(K)=-4e^2\int\frac{d^3\mathbf{p}}{(2\pi)^3}\hat{p}^i\partial^l f_e(\mathbf{p})\left(\delta^{jl}+\frac{\hat{p}^jk^l}{\omega-\mathbf{k}\cdot\hat{\mathbf{p}}+i\epsilon}\right), \tag{8}$$

where the electron distribution function $f_e(\mathbf{p})$ is, in principle, completely arbitrary. In what follows we will assume that $f_e(\mathbf{p})$ can be obtained from an isotropic distribution function by the rescaling of only one direction in momentum space. In practice this means that, given any isotropic distribution function $f_{e,\mathrm{iso}}(p)$, we can construct an anisotropic version by changing the argument of the isotropic distribution function

$$f_e(\mathbf{p})=N(\xi)f_{e,\mathrm{iso}}(\sqrt{\mathbf{p}^2+\xi(\mathbf{p}\cdot\hat{\mathbf{n}})^2}), \tag{9}$$

where $N(\xi)$ is a normalization constant, $\hat{\mathbf{n}}$ is the direction of the anisotropy and $\xi>-1$ is an adjustable anisotropy parameter. Note that $\xi>0$ corresponds to a contraction of the distribution along the $\hat{\mathbf{n}}$ direction whereas $-1<\xi<0$ corresponds to a stretching of the distribution along the $\hat{\mathbf{n}}$ direction.

The normalization constant, $N(\xi)$, can be determined by normalizing the distribution function to a fixed number density for all values of ξ

$$\int_{\mathbf{p}}f_{e,\mathrm{iso}}(p)=\int_{\mathbf{p}}f_e(\mathbf{p})=N(\xi)\int_{\mathbf{p}}f_{e,\mathrm{iso}}(\sqrt{\mathbf{p}^2+\xi(\mathbf{p}\cdot\hat{\mathbf{n}})^2}). \tag{10}$$

By performing a change of variables to $\tilde{p}$

$$\tilde{p}^2=p^2[1+\xi(\hat{\mathbf{p}}\cdot\hat{\mathbf{n}})^2], \tag{11}$$

on the right hand side we see that the normalization condition given in Eq. (10) requires that

$$N(\xi)=\sqrt{1+\xi}. \tag{12}$$

Making the same change of variables (11) also in (8) it is possible to integrate out the $|\tilde{p}|$ dependence giving

$$\Pi^{ij}(K)=m_D^2\sqrt{1+\xi}\int\frac{d\Omega}{4\pi}\hat{p}^i\frac{\hat{p}^l+\xi(\hat{\mathbf{p}}\cdot\hat{\mathbf{n}})n^l}{(1+\xi(\hat{\mathbf{p}}\cdot\hat{\mathbf{n}})^2)^2}\times\left(\delta^{jl}+\frac{\hat{p}^jk^l}{\omega-\mathbf{k}\cdot\hat{\mathbf{p}}+i\epsilon}\right), \tag{13}$$

where

$$m_D^2 = -\frac{2e^2}{\pi^2}\int_0^\infty dp p^2 \frac{df_{e,\mathrm{iso}}(p)}{dp}. \tag{14}$$

Note that in the analysis which follows we will assume that $f_{e,\mathrm{iso}}(p) = n_F(p) = [\exp(p/T)+1]^{-1}$, in which case $m_D^2 = e^2T^2/3$.

We can then decompose the self-energy into four structure functions

$$\mathbf{\Pi} = \alpha \mathbf{A} + \beta \mathbf{B} + \gamma \mathbf{C} + \delta \mathbf{D}, \tag{15}$$

which are determined by taking the following contractions:

$$\begin{aligned}
\hat{\mathbf{k}}\cdot\mathbf{\Pi}\cdot\hat{\mathbf{k}} &= \beta, \\
\tilde{\mathbf{n}}\cdot\mathbf{\Pi}\cdot\hat{\mathbf{k}} &= \tilde{n}^2 k\,\delta, \\
\tilde{\mathbf{n}}\cdot\mathbf{\Pi}\cdot\tilde{\mathbf{n}} &= \tilde{n}^2(\alpha+\gamma), \\
\mathrm{Tr}\,\mathbf{\Pi} &= 2\alpha+\beta+\gamma.
\end{aligned} \tag{16}$$

All four structure functions depend on m_D, ω, k, ξ, and $\hat{\mathbf{k}}\cdot\hat{\mathbf{n}}$. In the limit $\xi\to 0$ the structure functions α and β reduce to the isotropic hard-thermal-loop self-energies and γ and δ vanish

$$\begin{aligned}
\lim_{\xi\to 0}\alpha(K) &= \Pi_T(K) + \mathcal{O}(\xi), \\
\lim_{\xi\to 0}\beta(K) &= \frac{\omega^2}{k^2}\Pi_L(K) + \mathcal{O}(\xi), \\
\lim_{\xi\to 0}\gamma(K) &= \mathcal{O}(\xi), \\
\lim_{\xi\to 0}\delta(K) &= \mathcal{O}(\xi),
\end{aligned} \tag{17}$$

with

$$\Pi_T(K) = \frac{m_D^2}{2}\frac{\omega^2}{k^2}\left[1 - \frac{\omega^2-k^2}{2\omega k}\log\frac{\omega+k}{\omega-k}\right], \tag{18}$$

$$\Pi_L(K) = m_D^2\left[\frac{\omega}{2k}\log\frac{\omega+k}{\omega-k} - 1\right]. \tag{19}$$

The $\mathcal{O}(\xi)$ terms in Eq. (17) were determined analytically in Ref. [10].[1]

With these structure functions in hand we can construct the propagator $\Delta^{ij}(K)$ using the expressions from the previous section

$$\begin{aligned}
\Delta(K) = \Delta_A[\mathbf{A}-\mathbf{C}] + \Delta_G[(k^2-\omega^2+\alpha+\gamma)\mathbf{B} \\
+(\beta-\omega^2)\mathbf{C} - \delta\mathbf{D}],
\end{aligned} \tag{20}$$

where

$$\Delta_A^{-1}(K) = k^2 - \omega^2 + \alpha, \tag{21}$$

$$\begin{aligned}
\Delta_G^{-1}(K) = (k^2-\omega^2+\alpha+\gamma)(\beta-\omega^2) \\
- k^2\tilde{n}^2\delta^2.
\end{aligned} \tag{22}$$

III. ENERGY LOSS CALCULATION

In this section we compute the collisional energy loss of a heavy fermion propagating through an electromagnetic plasma which has an anisotropic momentum space electron distribution function. The starting point for the calculation is the same as in the isotropic case [12]. In these papers Braaten and Thoma calculated the energy loss of a heavy fermion for both QED and QCD. Here we will concentrate on QED but the extension to QCD is relatively straightforward. Note that there were previous calculations of the in-medium partonic energy loss [13–15]; however, the calculation of Braaten and Thoma was the first to present a systematic method for performing the complete order g calculation of this quantity.

The technique used by Braaten and Thoma was to consider independently the contributions from soft photon exchange ($q\sim m_D \sim eT$) and hard photon exchange ($q\sim T$). Each of these quantities is divergent with the soft contribution having a logarithmic UV divergence and the hard contribution having a logarithmic IR divergence. In their paper Braaten and Thoma found that if an arbitrary momentum scale q^* was introduced to separate the hard and soft regions then the dependence on this arbitrary scale vanished when the contributions are combined and the result obtained is finite.

Below we will use the same technique as Braaten and Thoma but we will show that if the resulting integrals are treated more carefully then the final result obtained by adding the soft and hard contributions does depend on q^*. However, in the weak-coupling limit $e \ll 1$ the dependence on q^* is small as long as $m_D \ll q^* \ll T$ and the Braaten-Thoma result is reproduced. Since the full result does depend on q^* we will need a prescription for fixing it. Here we will fix q^* using the ''principle of minimal sensitivity'' which in practice means that we minimize the energy loss with respect to q^* and evaluate at this point. We can then obtain a measurement of our theoretical uncertainty by varying q^* by a fixed amount around this point. Note that we have not attempted to estimate the uncertainty coming from the higher-order contributions to the heavy fermion energy loss. We present this variation in order to quantify the error made at leading order using the effective field theory approach which implicitly assumes a large scale separation.

In Secs. III A–III C we derive integral expressions for the soft and hard contributions to the energy loss and present some results for these in the limit of small anisotropies. We will also discuss complications which could arise due to the presence of plasma instabilities.

[1]Note that the normalization used in Ref. [10] is different than the normalization used here. The weak-anisotropy expansions for the normalization contained here can be obtained from the expressions contained in Ref. [10] by taking $m_D^2 \to \sqrt{1+\xi}\,m_D^2$ and re-expanding in ξ.

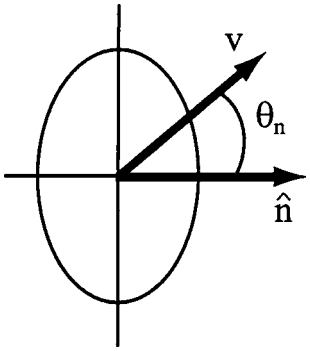

FIG. 1. Iso-surface for an oblate ($\xi>0$) electron distribution function showing the unit vector $\hat{\mathbf{n}}$, the particle three-velocity $\mathbf{v}$, and the angle θ_n defined by $\cos\theta_n \equiv \hat{\mathbf{v}}\cdot\hat{\mathbf{n}}$.

A. Soft part

For calculating the soft energy loss one can use classical field theory methods. The classical expression for parton energy loss per unit of time is

$$\left(\frac{\mathrm{d}W}{\mathrm{d}t}\right)_{\mathrm{soft}} = \mathrm{Re}\int d^3\mathbf{x}\mathbf{J}_{\mathrm{ext}}(X)\cdot\mathbf{E}_{\mathrm{ind}}(X), \tag{23}$$

where $X=(t,\mathbf{x})$, and $\mathbf{J}_{\mathrm{ext}}$ is the current induced by a test fermion propagating with velocity $\mathbf{v}$:

$$\mathbf{J}_{\mathrm{ext}}(X) = e\mathbf{v}\delta^{(3)}(\mathbf{x}-\mathbf{v}t),$$

$$\mathbf{J}_{\mathrm{ext}}(Q) = (2\pi)e\mathbf{v}\delta(\omega-\mathbf{q}\cdot\mathbf{v}), \tag{24}$$

with $Q=(\omega,\mathbf{q})$.

In order to make the geometry of the problem explicit in Fig. 1 we show an isosurface for an oblate ($\xi>0$) electron distribution function along with the unit vector $\hat{\mathbf{n}}$, the particle three-velocity $\mathbf{v}$, and the angle θ_n defined by $\cos\theta_n\equiv\hat{\mathbf{v}}\cdot\hat{\mathbf{n}}$. Using

$$E^i_{\mathrm{ind}}(Q) = i\omega[\Delta^{ij}(Q)-\Delta^{ij}_0(Q)]J^j_{\mathrm{ext}}(Q), \tag{25}$$

where Δ^{ij}_0 is the free propagator, and Fourier transforming to X we obtain

$$E^i_{\mathrm{ind}}(X) = ie\int \frac{d^3\mathbf{q}}{(2\pi)^3}(\mathbf{q}\cdot\mathbf{v})[\Delta^{ij}(Q) - \Delta^{ij}_0(Q)]v^j e^{i[\mathbf{q}\cdot\mathbf{x}-(\mathbf{q}\cdot\mathbf{v})t]}. \tag{26}$$

The above equation allows us to write Eq. (23) as

$$-\left(\frac{\mathrm{d}W}{\mathrm{d}t}\right)_{\mathrm{soft}} = e^2\mathrm{Im}\int \frac{d^3\mathbf{q}}{(2\pi)^3}(\mathbf{q}\cdot\mathbf{v})v^i[\Delta^{ij}(Q)-\Delta^{ij}_0(Q)]v^j. \tag{27}$$

The propagator can be expanded in our tensor basis and the contractions on the right hand side give

$$v^iA^{ij}v^j = v^2-(\hat{\mathbf{q}}\cdot\mathbf{v})^2,$$

$$v^iB^{ij}v^j = (\hat{\mathbf{q}}\cdot\mathbf{v})^2,$$

$$v^iC^{ij}v^j = (\tilde{\mathbf{n}}\cdot\mathbf{v})^2/\tilde{n}^2,$$

$$v^iD^{ij}v^j = 2(\mathbf{q}\cdot\mathbf{v})(\tilde{\mathbf{n}}\cdot\mathbf{v}), \tag{28}$$

so that together with $dW/dx = v^{-1}dW/dt$ we obtain

$$\begin{aligned}-\left(\frac{\mathrm{d}W}{\mathrm{d}x}\right)_{\mathrm{soft}} = \frac{e^2}{v}\mathrm{Im}\int \frac{d^3\mathbf{q}}{(2\pi)^3}\omega\left(\Delta_A(Q)-\frac{1}{q^2-\omega^2}\right)&\\ \times\left[v^2-\frac{\omega^2}{q^2}-\frac{(\tilde{\mathbf{n}}\cdot\mathbf{v})^2}{\tilde{n}^2}\right]&\\ +\omega\Delta_G(Q)\left[\frac{\omega^2}{q^2}(q^2-\omega^2+\alpha+\gamma)\right.&\\ \left.+(\beta-\omega^2)\frac{(\tilde{\mathbf{n}}\cdot\mathbf{v})^2}{\tilde{n}^2}-2\delta\omega(\tilde{\mathbf{n}}\cdot\mathbf{v})\right]&\\ +\frac{1}{\omega(q^2-\omega^2)}\left[\frac{\omega^2}{q^2}(q^2-\omega^2)-\omega^2\frac{(\tilde{\mathbf{n}}\cdot\mathbf{v})^2}{\tilde{n}^2}\right],&\end{aligned} \tag{29}$$

with $\omega=\mathbf{q}\cdot\mathbf{v}$. Performing some algebraic transformations and scaling out the momentum gives

$$\begin{aligned}\left(\frac{\mathrm{d}W}{\mathrm{d}x}\right)_{\mathrm{soft}} = \frac{e^2}{v}\mathrm{Im}\int \frac{d^3\mathbf{q}}{(2\pi)^3}\frac{\hat{\omega}}{q(1-\hat{\omega}^2)}&\\ \times\left[\frac{-\alpha}{(q^2-q^2\hat{\omega}^2+\alpha)}\left(v^2-\hat{\omega}^2-\frac{(\tilde{\mathbf{n}}\cdot\mathbf{v})^2}{\tilde{n}^2}\right)\right.&\\ \left.+\frac{q^2\mathcal{A}+\mathcal{B}}{q^4\mathcal{C}+q^2\mathcal{D}+\mathcal{E}}\right],&\end{aligned} \tag{30}$$

where

$$\mathcal{A} = (1-\hat{\omega}^2)^2\beta+\hat{\omega}^2\frac{(\tilde{\mathbf{n}}\cdot\mathbf{v})^2}{\tilde{n}^2}(\alpha+\gamma)-2\hat{\omega}(1-\hat{\omega}^2)(\tilde{\mathbf{n}}\cdot\mathbf{v})\hat{\delta},$$

$$\mathcal{B} = [(\alpha+\gamma)\beta-\tilde{\mathbf{n}}^2\hat{\delta}^2]\left(1-\hat{\omega}^2-\frac{(\tilde{\mathbf{n}}\cdot\mathbf{v})^2}{\tilde{n}^2}\right),$$

$$\mathcal{C} = -\hat{\omega}^2(1-\hat{\omega}^2),$$

$$\mathcal{D} = -\hat{\omega}^2(\alpha+\gamma)+(1-\hat{\omega}^2)\beta,$$

$$\mathcal{E} = (\alpha+\gamma)\beta-\tilde{\mathbf{n}}^2\hat{\delta}^2, \tag{31}$$

with $\hat{\omega}=\hat{\mathbf{q}}\cdot\mathbf{v}$ and $\hat{\delta}=q\delta$. With all the momentum dependence made explicit we can now perform the q integration to obtain

$$-\left(\frac{dW}{dx}\right)_{\text{soft}}=\frac{e^2}{v}\,\text{Im}\int\frac{d\Omega_q}{(2\pi)^3}\frac{\hat{\omega}}{(1-\hat{\omega}^2)}\times\left[-\alpha\frac{\left(v^2-\hat{\omega}^2-\frac{(\tilde{\mathbf{n}}\cdot\mathbf{v})^2}{\tilde{n}^2}\right)}{2(1-\hat{\omega}^2)}\times\ln\frac{q^{*2}(1-\hat{\omega}^2)+\alpha}{\alpha}+F(q^\star)-F(0)\right],\tag{32}$$

where

$$F(q)=\frac{\mathcal{A}}{4\mathcal{C}}\ln(-4\mathcal{C}(\mathcal{C}q^4+\mathcal{D}q^2+\mathcal{E}))+\frac{\mathcal{A}\mathcal{D}-2\mathcal{B}\mathcal{C}}{4\mathcal{C}\sqrt{\mathcal{D}^2-4\mathcal{C}\mathcal{E}}}\ln\frac{\sqrt{\mathcal{D}^2-4\mathcal{C}\mathcal{E}}+\mathcal{D}+2\mathcal{C}q^2}{\sqrt{\mathcal{D}^2-4\mathcal{C}\mathcal{E}}-\mathcal{D}-2\mathcal{C}q^2},\tag{33}$$

and we introduced an UV momentum cutoff q^* on the q integration. Note that, in principle, the presence of unstable modes would make the q integration divergent; however, this is not the case for the soft energy loss as we will discuss in Sec. III B.

1. Small-ξ limit

Using a linear expansion in the limit of small ξ one can obtain analytic expressions for the structure functions α, β, γ, and δ as given in Ref. [10]. A subsequent expansion of Eq. (32) to linear order in ξ gives

$$-\left(\frac{dW}{dx}\right)_{\text{soft, small}-\xi}=-\left\{\left(\frac{dW}{dx}\right)_{\text{soft,iso}}+\xi\left[\left(\frac{dW}{dx}\right)_{\text{soft},\xi_1}+\frac{(\mathbf{v}\cdot\hat{\mathbf{n}})^2}{v^2}\left(\frac{dW}{dx}\right)_{\text{soft},\xi_2}\right]\right\},\tag{34}$$

where

$$-\left(\frac{dW}{dx}\right)_{\text{soft,iso}}=\frac{e^2}{v^2}\,\text{Im}\int_{-v}^{v}\frac{d\hat{\omega}}{(2\pi)^2}\hat{\omega}\times\left[-\frac{v^2-\hat{\omega}^2}{2(1-\hat{\omega}^2)^2}\Pi_T\ln\frac{(1-\hat{\omega}^2)q^{*2}+\Pi_T}{\Pi_T}-\frac{\Pi_L}{2}\ln\frac{q^{*2}-\Pi_L}{-\Pi_L}\right]\tag{35}$$

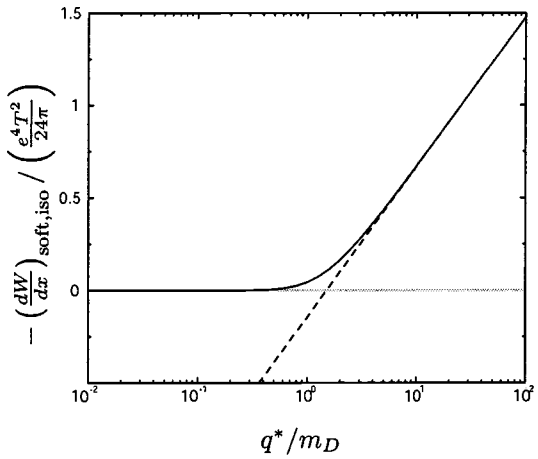

FIG. 2. Isotropic energy loss of the soft part (full line) as a function of q^*/m_D for $v=0.5$ compared to the result from Braaten and Thoma (dashed line).

is the isotropic result, which—assuming $q^*\gg m_D$—corresponds to the result from Braaten and Thoma when inserting the explicit form of $\Pi_T(\hat{\omega})$ and $\Pi_L(\hat{\omega})$ from Eqs. (18) and (19). The form of the contributions $(dW/dx)_{\text{soft},\xi_1}$ and $(dW/dx)_{\text{soft},\xi_2}$ resembles that of $(dW/dx)_{\text{soft,iso}}$, but since they consist of many more terms than the isotropic contribution we refrain from giving them here explicitly.

Note that by scaling out the Debye mass m_D from the self-energy functions, the contributions $(dW/dx)_{\text{soft,iso}}$, $(dW/dx)_{\text{soft},\xi_1}$ and $(dW/dx)_{\text{soft},\xi_2}$ depend on the particle velocity v, the ratio q^*/m_D, and an overall multiplicative factor of $e^2m_D^2$ only. The direction of the heavy fermion enters the whole result Eq. (34) only through the explicit term $(\mathbf{v}\cdot\hat{\mathbf{n}})^2/v^2$ in the small ξ limit.

2. Behavior of the soft part

The isotropic result for the soft part, Eq. (35) (corresponding to the result obtained in Ref. [14]), is shown in Fig. 2 together with the Braaten-Thoma result from Ref. [12] for $v=0.5$. As can be seen, the results are identical for large q^*/m_D, while for small q^*/m_D the Braaten-Thoma result becomes negative whereas the full result obtained by numerical integration of Eq. (35) is positive for all values of q^*/m_D.

In Fig. 3 we show the function $-(dW/dx)_{\text{soft},\xi_2}$ which controls the directional dependence of the soft part of the energy loss for small ξ. As can be seen from this figure the function is negative for small q^*/m_D but becomes positive at a velocity-dependent value of q^*/m_D. The value of q^*/m_D where $(dW/dx)_{\text{soft},\xi_2}=0$ is of special interest here since it signals the point at which the directional dependence of the energy loss changes. The value of q^*/m_D obtained using the principle of minimal sensitivity is a function of the velocity and coupling constant and therefore we expect a non-trivial dependence on these parameters. For $\xi>0$ this means that as the coupling constant is increased from zero for fixed v that

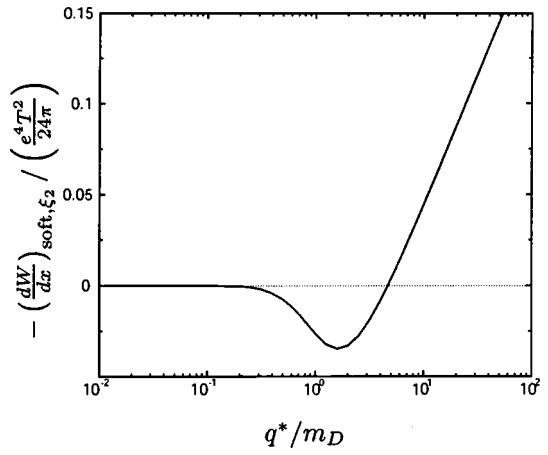

FIG. 3. The contribution $-(dW/dx)_{\text{soft},\xi_2}$ as a function of q^*/m_D for $v=0.5$.

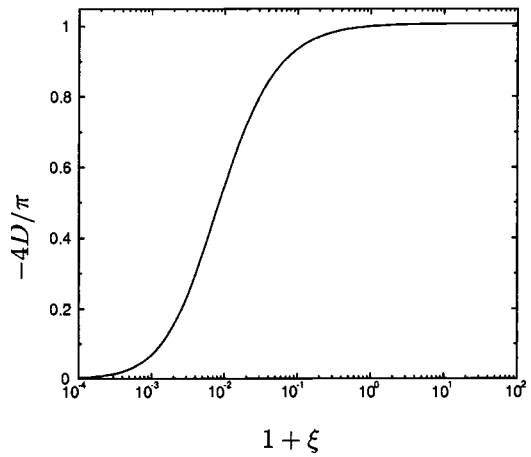

FIG. 4. Coefficient D as a function of ξ for $\theta_n=1.5$.

at first the energy loss will be peaked along $\hat{\mathbf{n}}$ but will eventually become peaked transverse to $\hat{\mathbf{n}}$. The value of the coupling at which this change in the directional dependence occurs increases as the velocity of the fermion increases. For the exact expression given by Eq. (32) the results obtained in the small ξ limit hold qualitatively but quantitatively the predictions differ considerably once ξ becomes large.

3. Large-ξ limit

In the limit $\xi\to\infty$ one finds that the anisotropic distribution function turns into a specific case of Eq. (1),

$$\lim_{\xi\to\infty}\sqrt{1+\xi}n_F(p\sqrt{1+\xi(\hat{\mathbf{p}}\cdot\hat{\mathbf{n}})^2}) = \delta(\hat{\mathbf{p}}\cdot\hat{\mathbf{n}})\int_{-\infty}^{\infty}dx n_F(p\sqrt{1+x^2}), \tag{36}$$

where the remaining integral representing $F(p_\perp)$ in Eq. (1) can be evaluated analytically to be a sum over Bessel functions. Following Ref. [11] it is then possible to evaluate the structure functions analytically. The result for the soft part of the energy loss is then given by Eq. (32) with the general structure functions replaced by their large-ξ expressions. For large values of ξ, the general result for the soft part converges towards the limiting result, as it should.

B. Dynamical shielding of plasma instabilities

As shown previously [5–11] in systems in which the distribution function is anisotropic in momentum space there exist unstable modes which could potentially make physical quantities incalculable within a perturbative framework [16]. However, we will show in this section that in the case of the energy loss the singularities induced by the presence of these plasma instabilities are ''shielded'' and are therefore rendered safe. To see this one need only consider the contribution from the Δ_A propagator to Eq. (30) which is schematically given by

$$\left(\frac{dW}{dx}\right)_{\text{A, soft}} \sim \text{Im}\int d\Omega\int qdq\,\frac{\hat{\omega}}{(1-\hat{\omega}^2)}\,\frac{-\alpha}{(q^2-q^2\hat{\omega}^2+\alpha)}. \tag{37}$$

The possibility of singularities arise because in the static limit the structure function α is negative-valued which can result in singularities along the integration path which are unregulated. However, in the limit $\omega\to 0$ the structure function α has the form

$$\lim_{\omega\to 0}\alpha(\omega,q)=M^2(-1+iD\hat{\omega})+\mathcal{O}(\omega^2), \tag{38}$$

where M and D depend on the angle of propagation with respect to the anisotropy vector and the strength of the anisotropy.

Ignoring the $\mathcal{O}(\omega)$ contribution above we see that a singularity in the integrand can arise at the point $q=M$ when $\hat{\omega}\to 0$. However, including the $\mathcal{O}(\omega)$ contribution we see that the combination of the power of $\hat{\omega}$ in the numerator and the presence of a contribution proportional to $\hat{\omega}$ in α together render the singularity finite at this point as long as D is non-vanishing

$$\lim_{\hat{\omega}\to 0}\lim_{q\to M}\frac{\hat{\omega}}{q^2-q^2\hat{\omega}^2+M^2(-1+iD\hat{\omega})} \to\frac{1}{M^2(\hat{\omega}+iD)}\to-\frac{i}{M^2D}. \tag{39}$$

Therefore, the q integration can safely be performed. Of course, the integrand may change rapidly in this region so it should be treated carefully when numerically evaluating the integral. Note that this is similar to dynamical screening of the magnetic sector of finite temperature QCD. In fact, in the isotropic limit, the coefficient D approaches the well-known value of $-\pi/4$ which is due to Landau damping. Unfortunately for anisotropic systems it is difficult to prove that the coefficient D is non-vanishing for all values of the propagation angle and anisotropy strength. However, we can evalu-

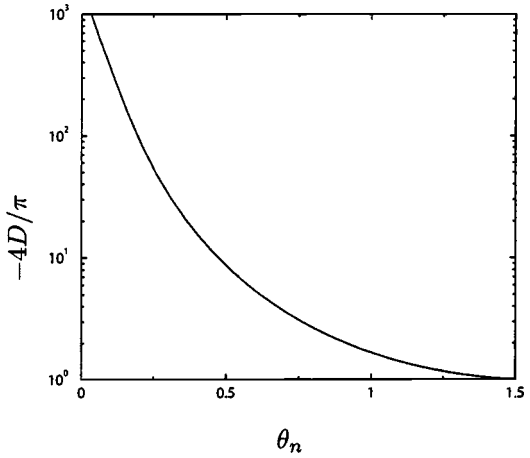

FIG. 5. Coefficient D as a function of θ_n for $\xi=100$.

ate D analytically in the weak-anisotropy limit and numerically for general ξ and in both cases we find that D is non-vanishing.

In the weak-anisotropy limit we can derive analytic expressions for all of the structure functions as shown in Ref. [10]. To linear order in ξ the structure function α becomes

$$\lim_{\hat{\omega}\to 0}\lim_{\xi\to 0}\alpha = m_D^2\left[-\frac{\xi}{6}(1+\cos 2\theta_n) - \frac{i\pi}{4}\hat{\omega}\left(1+\frac{3\xi}{4}(1+\cos 2\theta_n)\right)\right], \quad (40)$$

where θ_n is the angle of propagation with respect to the anisotropy vector $\hat{\mathbf{n}}$. Therefore, in the weak-anisotropy limit D is non-vanishing for all $\xi>0$. For $\xi<0$, the Δ_A mode is stable so there is no singularity to be concerned about. At higher orders in the weak-anisotropy expansion the picture becomes slightly more complicated but is still consistent with D being non-vanishing.

For large values of ξ we cannot rely on a weak-anisotropy expansion so we have to resort to numerical determination of D. In Fig. 4 we plot the dependence of D on ξ for $\theta_n=1.5$ and in Fig. 5 we plot the dependence of D on θ_n for $\xi=100$. As can be seen from these figures, D is non-vanishing for all values of ξ and θ_n shown. Beyond what we have plotted, we have calculated D for numerous values of ξ and θ_n and in every case we find that D is non-vanishing. We are therefore reasonably confident that D is in general a non-vanishing quantity and therefore the singularities which could come from the unstable modes are dynamically shielded and thereby rendered safe in the energy loss calculation. Note that similar arguments can be made to show that the singularities coming from the Δ_G contribution to Eq. (30) are also dynamically shielded.

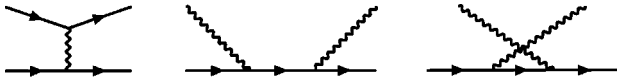

FIG. 6. Tree-level Feynman diagrams for the scattering processes $e^-\mu\to e^-\mu$ and $\gamma\mu\to\gamma\mu$. Note that the second two diagrams cancel with each other so that in QED only the first diagram contributes to the hard energy loss.

C. Hard part

The expression for the hard contribution to the energy loss for an arbitrary electron distribution function $f_e(\mathbf{p})$ is obtained by summing the tree level diagrams shown if Fig. 6. Assuming $v\gg T/E$, performing the Dirac traces, and summing over spins, the result can be reduced to [12]

$$-\left(\frac{dW}{dx}\right)_{\rm hard} = \frac{4\pi e^4}{v}\int\frac{d^3\mathbf{k}}{(2\pi)^3}\frac{f_e(\mathbf{k})}{k}\int\frac{d^3\mathbf{k}'}{(2\pi)^3}\frac{1-f_e(\mathbf{k}')}{k'} \times\delta(\omega-\mathbf{v}\cdot\mathbf{q})\Theta(q-q^*)\frac{\omega}{(\omega^2-q^2)^2} \times\left[2(k-\mathbf{v}\cdot\mathbf{k})(k'-\mathbf{v}\cdot\mathbf{k}')+\frac{1-v^2}{2}(\omega^2-q^2)\right], \quad (41)$$

where $\omega=k'-k$ and $\mathbf{q}=\mathbf{k}'-\mathbf{k}$, and we have introduced an infrared cutoff q^* on the q integration. The term involving the product $f_e(\mathbf{k})f_e(\mathbf{k}')$ vanishes since the integrand is odd under the interchange of $\mathbf{k}$ and $\mathbf{k}'$. Redefining the origin of the $\mathbf{k}'$ integration so that it becomes an integration over $\mathbf{q}$, we have

$$-\left(\frac{dW}{dx}\right)_{\rm hard} = \frac{e^4}{2\pi^2 v}\int\frac{d^3\mathbf{k}}{(2\pi)^3}\frac{f_e(\mathbf{k})}{k}\int_{q^*}^{\infty}q^2dq \times\int d\Omega_q\frac{\delta(\omega-\mathbf{v}\cdot\mathbf{q})}{|\mathbf{q}+\mathbf{k}|}\frac{\omega}{(\omega^2-q^2)^2} \times\left[2(k-\mathbf{v}\cdot\mathbf{k})(\omega+k-\mathbf{v}\cdot\mathbf{k}-\mathbf{v}\cdot\mathbf{q}) + \frac{1-v^2}{2}(\omega^2-q^2)\right], \quad (42)$$

where now $\omega=|\mathbf{q}+\mathbf{k}|-k$. Choosing $\mathbf{v}$ to be the z axis for the $\mathbf{q}$ and $\mathbf{k}$ integration we can rewrite the delta function as

$$\delta(|\mathbf{q}+\mathbf{k}|-k-\mathbf{v}\cdot\mathbf{q}) = \frac{\delta(\phi_q-\phi_0)\Theta(k+\mathbf{v}\cdot\mathbf{q})2|\mathbf{q}+\mathbf{k}|}{q\sqrt{4k^2\sin^2\theta_k\sin^2\theta_q-[q(1-v^2\cos^2\theta_q)+2\cos\theta_q(k\cos\theta_k-kv)]^2}}, \quad (43)$$

where ϕ_0 is the solution of the equation

$$\cos(\phi_0-\phi_k)=-\frac{q(1-v^2\cos^2\theta_q)+2\cos\theta_q(k\cos\theta_k-kv)}{2k\sin\theta_k\sin\theta_q}. \tag{44}$$

The ϕ_q integration is then straightforward and we obtain

$$\begin{aligned}-\left(\frac{dW}{dx}\right)_{\text{hard}}=&\frac{e^4}{2\pi^2 v}\int\frac{d^3\mathbf{k}}{(2\pi)^3}\frac{f_e(\mathbf{k})}{k}\int_{q^*}^{\infty}qdq\int_{-1}^{1}d\cos\theta_q 4\Theta(k+vq\cos\theta_q)\\&\times\frac{\Theta(4k^2\sin^2\theta_k\sin^2\theta_q-[q(1-v^2\cos^2\theta_q)+2\cos\theta_q(k\cos\theta_k-kv)]^2)}{\sqrt{4k^2\sin^2\theta_k\sin^2\theta_q-[q(1-v^2\cos^2\theta_q)+2\cos\theta_q(k\cos\theta_k-kv)]^2}}\frac{\omega}{(\omega^2-q^2)^2}\\&\times\left[2(k-\mathbf{v}\cdot\mathbf{k})^2+\frac{1-v^2}{2}(\omega^2-q^2)\right],\end{aligned} \tag{45}$$

where $\omega=vq\cos\theta_q$ and we have included a factor of 2 because of the symmetry $\phi_0\leftrightarrow 2\pi-\phi_0$. Setting $f_{e,\text{iso}}(k)=n_F(k)$ and scaling $k=qz$ one can perform the q integration to obtain

$$\begin{aligned}-\left(\frac{dW}{dx}\right)_{\text{hard}}=&\frac{8e^4(\hat{q}^*)^2T^2\sqrt{1+\xi}}{(2\pi)^5 v}\int_0^{\infty}zdz\int_{-1}^{1}d\cos\theta_k\left[\int_0^{2\pi}d\phi_k F_1[\hat{q}^*z\sqrt{1+\xi(n_x\sin\theta_k\cos\phi_k+n_z\cos\theta_k)^2}]\right]\\&\times\left\{\int_{-1}^{1}d\cos\theta_q\Theta(z+v\cos\theta_q)\frac{\Theta(4z^2\sin^2\theta_k\sin^2\theta_q-[1-v^2\cos^2\theta_q+2\cos\theta_q z(\cos\theta_k-v)]^2)}{\sqrt{4z^2\sin^2\theta_k\sin^2\theta_q-[1-v^2\cos^2\theta_q+2\cos\theta_q z(\cos\theta_k-v)]^2}}\right.\\&\left.\times\frac{v\cos\theta_q}{(v^2\cos^2\theta_q-1)^2}\left[2z^2(1-v\cos\theta_k)^2+\frac{1-v^2}{2}(v^2\cos^2\theta_q-1)\right]\right\},\end{aligned} \tag{46}$$

where $\hat{q}^*=q^*/T$,

$$F_1(x)=\frac{x\ln(1+\exp(-x))-\text{Li}_2(-\exp(-x))}{x^2}, \tag{47}$$

and $n_z=\hat{\mathbf{n}}\cdot\hat{\mathbf{v}}$ with $1=n_x^2+n_z^2$. To obtain the final result for the hard contribution to the energy loss the remaining integrations have to be performed numerically.

1. Small-ξ limit

For small ξ we use Eq. (42) and scale out the ξ dependence using Eq. (9) and substituting $k^2\to k^2[1+\xi(\hat{\mathbf{k}}\cdot\hat{\mathbf{n}})^2]$ and $q^2\to q^2[1+\xi(\hat{\mathbf{k}}\cdot\hat{\mathbf{n}})^2]$. Performing a linear expansion in ξ then gives

$$\begin{aligned}-\left(\frac{dW}{dx}\right)_{\text{hard, small}\xi}=&\frac{e^4}{2\pi^2 v}\int_0^{\infty}dk f_{e,\text{iso}}(k)\\&\times\left\{\int_{q^*}^{\infty}dq\left[g_1(q)-\xi\left(g_2(q)-\frac{g_1(q)}{2}\right)\right]\right.\\&\left.-\frac{\xi}{2}q^*g_2(q^*)\right\},\end{aligned} \tag{48}$$

where

$$\begin{aligned}g_1(q)=&\int d\Omega_q\int\frac{d\Omega_k}{4\pi}q^2\frac{\delta(\omega-\mathbf{v}\cdot\mathbf{q})}{|\mathbf{q}+\mathbf{k}|}\frac{\omega}{\omega^2-q^2}\\&\times\left[2(k-\mathbf{v}\cdot\mathbf{k})^2+\frac{1-v^2}{2}(\omega^2-q^2)\right]\end{aligned}$$

$$\begin{aligned}g_2(q)=&\int d\Omega_q\int\frac{d\Omega_k}{4\pi}q^2(\hat{\mathbf{k}}\cdot\hat{\mathbf{n}})^2\frac{\delta(\omega-\mathbf{v}\cdot\mathbf{q})}{|\mathbf{q}+\mathbf{k}|}\frac{\omega}{\omega^2-q^2}\\&\times\left[2(k-\mathbf{v}\cdot\mathbf{k})^2+\frac{1-v^2}{2}(\omega^2-q^2)\right].\end{aligned} \tag{49}$$

Taking $\mathbf{q}$ as the z direction makes the $d\Omega_k$ integration straightforward but still algebraically intensive for the g_2 contribution because of the extra dependence on $\hat{\mathbf{k}}\cdot\hat{\mathbf{n}}$. Next we rotate the coordinate system so that $\mathbf{v}$ becomes the new z direction and $\hat{\mathbf{n}}$ lies in the x-z plane for the $d\Omega_q$ integration; the polar integration is then also straightforward whereas for the azimuthal integration the limits coming from the delta function in Eq. (49) are somewhat non-trivial. Nevertheless, by scaling $k=qz$ one can perform the q integration to obtain

$$-\left(\frac{dW}{dx}\right)_{\text{hard, small}\xi} = \frac{e^4(q^*)^2}{2\pi^2 v}\int_0^\infty \frac{dz}{2\pi^2} z \times\left[F_1(\hat{q}^* z)\left[g_1(1)-\xi\left(g_2(1)-\frac{g_1(1)}{2}\right)\right] - \frac{\xi}{2} f_{\text{iso}}(\hat{q}^* z) g_2(1)\right], \quad (50)$$

where $\hat{q}^* = q^*/T$,

$$g_1(1) = \frac{\pi}{zv}\int_{|1-z|-z}^1 d\omega\Theta(v^2-\omega^2)\omega\left[\frac{3\omega^2}{4}-\frac{v^2}{4}+3z(z+\omega) - \frac{1-v^2}{2}\frac{1}{1-\omega^2}-(1-v^2)\frac{z(z+\omega)}{1-\omega^2}\right], \quad (51)$$

and the exact form of g_2 is similar to g_1 but involves many more terms so we have refrained from giving an explicit expression. The integration over ω can then be performed analytically using

$$\int_0^\infty dz\int_{|1-z|-z}^1 d\omega\Theta(v^2-\omega^2) = \int_{(1-v)/2}^{(1+v)/2} dz\int_{1-2z}^v d\omega + \int_{(1+v)/2}^\infty dz\int_{-v}^v d\omega, \quad (52)$$

but the remaining integral over z has to be performed numerically. The final result to linear order in ξ can then be written as

$$-\left(\frac{dW}{dx}\right)_{\text{hard, small}\xi} = -\left\{\left(\frac{dW}{dx}\right)_{\text{hard,iso}} + \xi\left[\left(\frac{dW}{dx}\right)_{\text{hard},\xi_1} + \frac{(\mathbf{v}\cdot\hat{\mathbf{n}})^2}{v^2}\left(\frac{dW}{dx}\right)_{\text{hard},\xi_2}\right]\right\}, \quad (53)$$

where $(dW/dx)_{\text{hard,iso}}$ is given by Eq. (50) with $\xi=0$.

2. Behavior of the hard part

In Fig. 7 we show the result for the isotropic ($\xi=0$) result for the hard part compared to the Braaten-Thoma result from Ref. [12]. Similar to what we found for the soft part, the two results are identical for very small $\hat{q}^*$, while for large $\hat{q}^*$ the Braaten-Thoma result becomes negative and our result is positive for all values of $\hat{q}^*$.

In Fig. 8 we plot the function $-(dW/dx)_{\text{hard},\xi_2}$, which controls the directional dependence of the hard part of the energy loss. As was the case with the soft part, $(dW/dx)_{\text{hard},\xi_2}=0$ for a velocity-dependent value of q^*. Again, in practice, this means that the directional dependence of the hard energy loss changes as the coupling constant is increased.

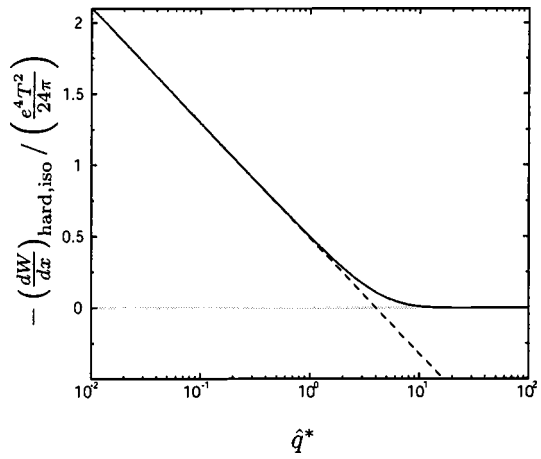

FIG. 7. Isotropic energy loss of the hard part (full line) as a function of $\hat{q}^*$ for $v=0.5$ compared to the result from Braaten and Thoma (dashed line).

3. Large-ξ limit

Using the explicit form (36) for f_e one can do the $d\phi_k$ integration in Eq. (45) by rewriting

$$\delta(\hat{\mathbf{k}}\cdot\hat{\mathbf{n}}) = \frac{\delta(\phi_k-\phi_0)}{\sqrt{n_x^2-\cos^2\theta_k}}, \quad \cos\theta_0 = -\frac{\cos\theta_k n_z}{\sin\theta_k n_x}. \quad (54)$$

After scaling $\cos\theta_k \to n_x\cos\theta_k$ and doing the q integration the remaining integrals take the form

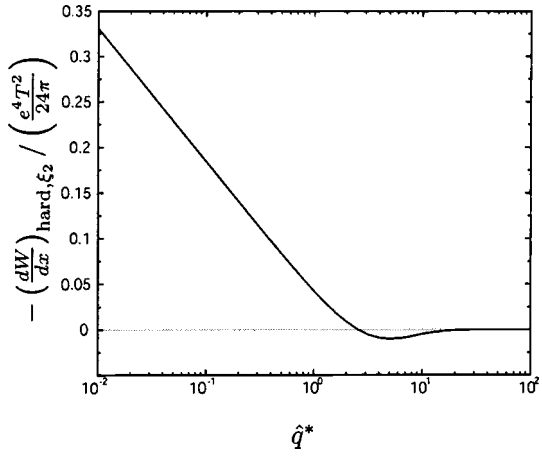

FIG. 8. The contribution $-(dW/dx)_{\text{hard},\xi_2}$ as a function of $\hat{q}^*$ for $v=0.5$.

$$-\left(\frac{dW}{dx}\right)_{\text{hard}} = \frac{32e^4(\hat{q}^*)^2T^2}{(2\pi)^5 v}\int_0^\infty z\,dz\int_0^\infty dx F_1(\hat{q}^* z\sqrt{1+x^2})\int_{-1}^{1} d\cos\theta_k \frac{1}{\sqrt{1-\cos^2\theta_k}}\int_{-1}^{1} d\cos\theta_q$$
$$\times\left\{\Theta(z+v\cos\theta_q)\frac{\Theta(4z^2(1-n_x^2\cos^2\theta_k)\sin^2\theta_q-[1-v^2\cos^2\theta_q+2\cos\theta_q z(n_x\cos\theta_k-v)]^2)}{\sqrt{4z^2(1-n_x^2\cos^2\theta_k)\sin^2\theta_q-[1-v^2\cos^2\theta_q+2\cos\theta_q z(n_x\cos\theta_k-v)]^2}}\right.$$
$$\left.\times\frac{v\cos\theta_q}{(v^2\cos^2\theta_q-1)^2}\left[2z^2(1-vn_x\cos\theta_k)^2+\frac{1-v^2}{2}(v^2\cos^2\theta_q-1)\right]\right\}, \tag{55}$$

which after evaluation then give the result for the hard part of the energy loss in the large-ξ limit.

IV. NUMERICAL EVALUATION

A. Isotropic case

In the isotropic case, the total collisional energy loss is obtained by adding Eqs. (35) and (50) with $\xi=0$,

$$\left(\frac{dW}{dx}\right)_{\text{iso}} = \left(\frac{dW}{dx}\right)_{\text{iso,soft}} + \left(\frac{dW}{dx}\right)_{\text{iso,hard}}. \tag{56}$$

In general the isotropic energy loss is a function of the electromagnetic coupling e, the velocity of the particle v, the temperature T, and the momentum separation scale q^*.

In principle q^* should be an arbitrary quantity in the range $e \ll q^*/T \ll 1$ which is possible in the weak-coupling limit. Choosing $e=0.01$ and plotting $-dW/dx$ as a function of $\hat{q}^*=q^*/T$ at fixed v and T we find the result shown in Fig. 9. From this figure we can see that the energy loss develops a plateau where the value is essentially identical to the result obtained by Braaten and Thoma; however, outside the plateau the function rises logarithmically with $\hat{q}^*$. For higher coupling ($e \gtrsim 0.5$) the plateau shrinks rapidly to a minimum which can be seen in Fig. 10. We fix $\hat{q}^*$ by minimizing the energy loss with respect to $\hat{q}^*$.

In Fig. 11 we compare our result with the result obtained by Braaten and Thoma for $e=0.3$. The Braaten-Thoma result is shown as a dashed line and our result is shown as a gray band. The band corresponds to the variation we obtain in our final result when varying the scale $\hat{q}^*$ by a factor of two around the central value (minimum). Note that the choice of varying by a factor of two is completely arbitrary. We could have easily chosen a smaller variation; however, we have chosen to be conservative here and vary $\hat{q}^*$ by a factor of two. As can be seen from this figure, for $e=0.3$, the corrections to the Braaten-Thoma result are small; however, for larger couplings the band obtained by varying $\hat{q}^*$ by a factor of two can be quite large. The size of these bands gives us an estimate of the theoretical uncertainty present in the calculation.

B. Anisotropic case

In the general anisotropic case we have to numerically evaluate the integrals contained in Eqs. (32) and (46) and add these to obtain the total energy loss

$$\left(\frac{dW}{dx}\right) = \left(\frac{dW}{dx}\right)_{\text{soft}} + \left(\frac{dW}{dx}\right)_{\text{hard}}. \tag{57}$$

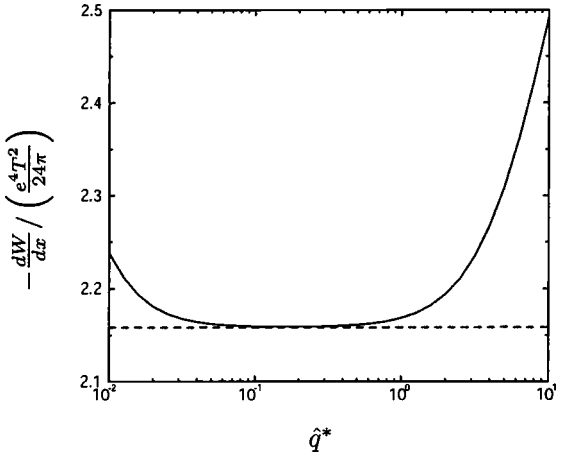

FIG. 9. Energy loss as a function of $\hat{q}^*$ for $v=0.5$ and $e=0.01$. The dashed line corresponds to the result from Braaten and Thoma.

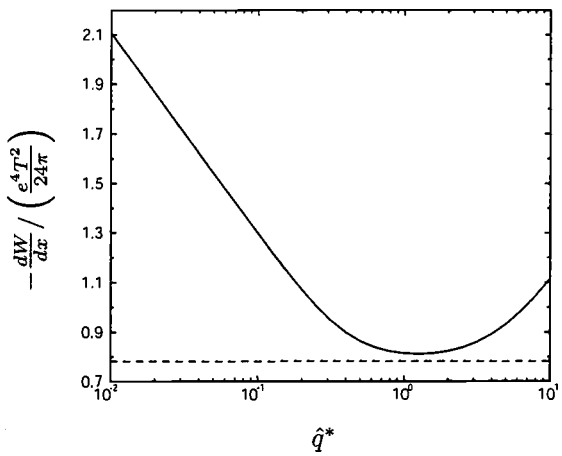

FIG. 10. Energy loss as a function of $\hat{q}^*$ for $v=0.5$ and $e=0.5$. The dashed line corresponds to the result from Braaten and Thoma.

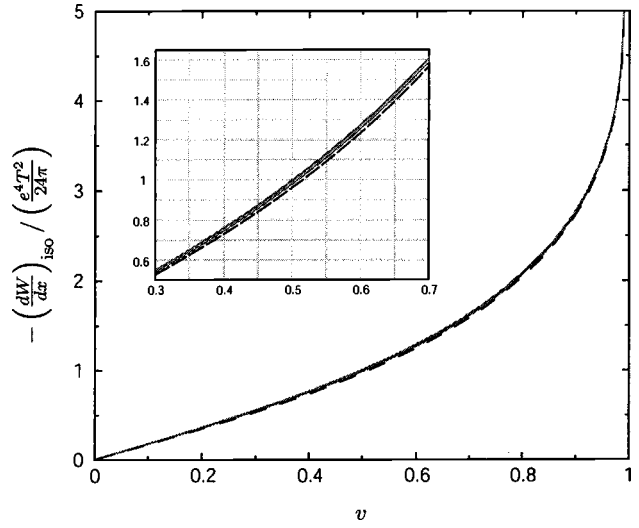

FIG. 11. Isotropic energy loss as a function of the electron velocity v for $e=0.3$. The dashed line is the Braaten-Thoma result. The gray band indicates the variation of the result obtained by varying q^* by a factor of two around the central value. Inset is an enlarged version of the region $0.3<v<0.7$.

In addition to v and e the anisotropic energy loss also depends on the anisotropy parameter ξ and the angle of propagation with respect to the anisotropy vector θ_n. Note that for every value of v, e, ξ, and θ_n there is a non-trivial consistency check between the hard and soft contributions, namely that the coefficients of $\log\hat{q}^*$ have to be equal and opposite for small $\hat{q}^*$ and large $\hat{q}^*$, respectively. In every case that we have examined we find that these coefficients match to a part in 10^{-4}, which can be further improved by increasing the target integration accuracy.

As in the isotropic case we find that for small coupling there is a plateau for $e \ll \hat{q}^* \ll 1$ and our final result is obtained by finding the minimum of the energy loss as a function of $\hat{q}^*$. This corresponds to the point at which the result is minimally sensitive to $\hat{q}^*$. As before, we can then obtain an estimate of the uncertainty in our prediction by varying $\hat{q}^*$ by a factor of two around the point of minimal sensitivity. Note that by using this method the central value of $\hat{q}^*$ always serves as a lower-bound on the prediction.

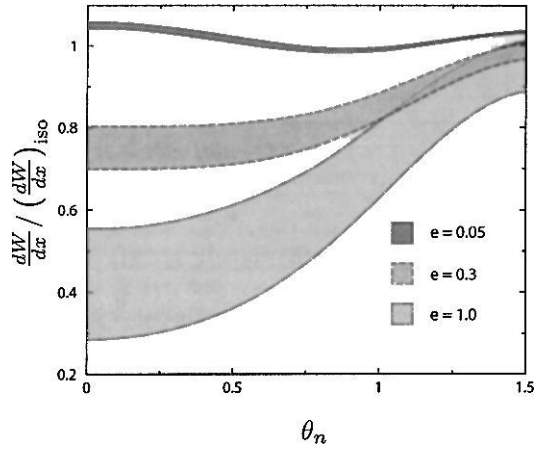

FIG. 13. Scaled energy loss as a function of the angle of propagation with respect to $\hat{\mathbf{n}}$ for $v=0.3$ and $\xi=10$.

In Figs. 12–17 we plot the θ_n dependence of the resulting anisotropic energy loss for $v=\{0.3,0.5,0.7\}$, $e=\{0.05,0.3,1.0\}$, and $\xi=\{1,10\}$ scaled by the corresponding isotropic energy loss. For $e=0.05$ we see that for all three values of the velocity the energy loss is larger along the direction of the anisotropy then transverse to it. For the physical value of electromagnetic coupling constant, $e=0.3$, we find that directional dependence of the energy loss depends on the velocity and the strength of the anisotropy. For $v=0.3$ and $\xi=1$ the result is almost independent of the direction of propagation but if the anisotropy is stronger ($\xi=10$) then the energy loss is less in the direction of the anisotropy than transverse to it. Note that this is consistent with the results obtained in the small-ξ limit in Secs. III A 2 and III C 2. For larger velocities we find that the energy loss along the direction of the anisotropy is higher than transverse to it; however, if the coupling constant is increased to a large enough value then the trend will reverse, as was the case for smaller velocities. Note that for $v \gtrsim 0.5$ the coupling constant required to reverse the trend is extremely large.

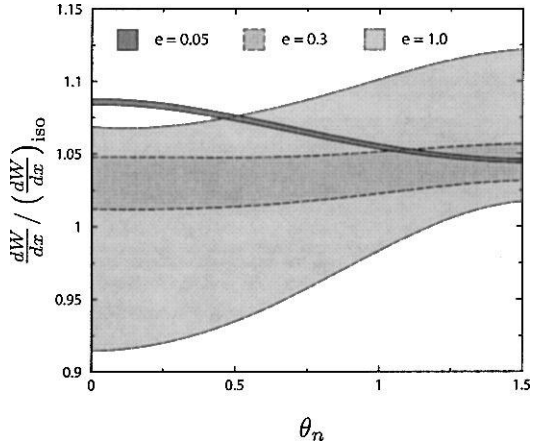

FIG. 12. Scaled energy loss as a function of the angle of propagation with respect to $\hat{\mathbf{n}}$ for $v=0.3$ and $\xi=1$.

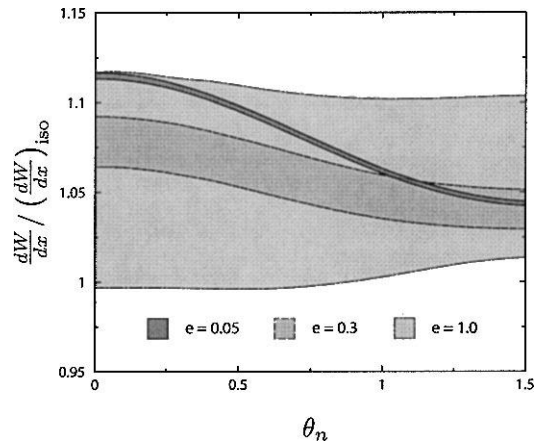

FIG. 14. Scaled energy loss as a function of the angle of propagation with respect to $\hat{\mathbf{n}}$ for $v=0.5$ and $\xi=1$.

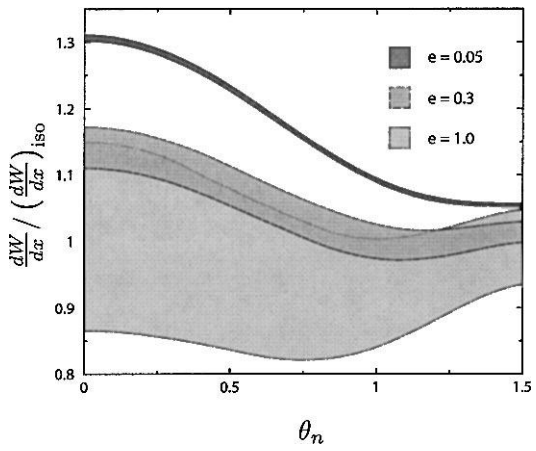

FIG. 15. Scaled energy loss as a function of the angle of propagation with respect to $\hat{\mathbf{n}}$ for $v=0.5$ and $\xi=10$.

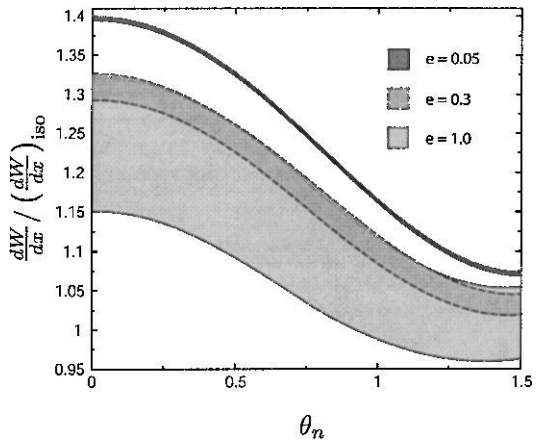

FIG. 17. Scaled energy loss as a function of the angle of propagation with respect to $\hat{\mathbf{n}}$ for $v=0.7$ and $\xi=10$.

In the most extreme case shown here in Fig. 17 for which $v=0.7$ and $\xi=10$ we see that for all values of the coupling constant shown the energy loss varies by 20–25 %, depending on whether the fermion is propagating along the direction of the anisotropy or transverse to it. For larger values of the velocity and anisotropy parameter the directional dependence of the energy loss increases.

In Fig. 18 we plot the dependence of the energy loss normalized to the isotropic result for $\xi=1$, $e=0.3$, and $\theta_n=\{0,1.5\}$ as a function of the velocity v. From this figure we see that for fixed e and ξ the angular dependence (forward peaked versus transversely peaked) changes as the velocity is increased with the energy loss being transversely-peaked for small velocities and forward-peaked for large velocities. For the largest velocity shown in this figure we see that for $\xi=1$ the effect is on the order of 10%.

In Fig. 19 we plot the dependence of the energy loss for $v=0.5$, $e=0.3$, and $\theta_n=\{0,1.5\}$ as a function of ξ. Additionally, we have included results obtained by taking the large-ξ limit by lines on the right hand side of the plot frame. As can be seen from this figure for $\xi>0$ we find that the difference between the forward and transverse energy loss saturates at approximately 25% in the large ξ limit. For $\xi<0$ we see that for both angles shown the energy loss approaches zero but the difference between the forward and transverse energy loss is still quite large at $\xi=-0.99$. Therefore, it is possible that the presence of momentum-space anisotropies in the electron distribution function could lead to a rather significant experimental effect.

V. CONCLUSIONS

In this paper we have derived integral expressions for the collisional energy loss of a heavy fermion propagating through a QED plasma for which the electron distribution function is anisotropic in momentum space. We then numerically evaluated the resulting integrals and studied the dependence of the heavy fermion energy loss on the angle of propagation, degree of momentum-space anisotropy, and coupling constant. We have shown that the techniques used in the isotropic case can be straightforwardly extended to the anisotropic case. We have also discussed how problems due to unstable soft photonic modes are avoided in the case of the energy loss.

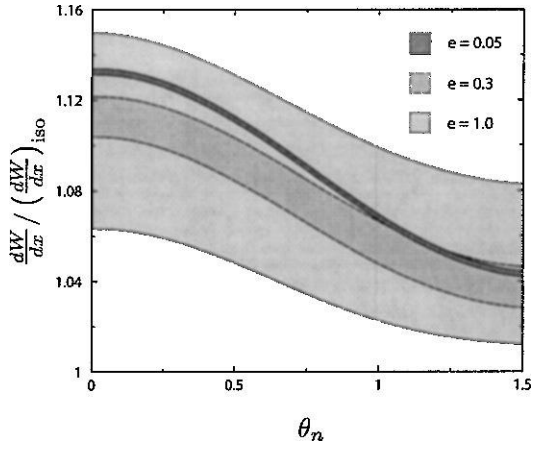

FIG. 16. Scaled energy loss as a function of the angle of propagation with respect to $\hat{\mathbf{n}}$ for $v=0.7$ and $\xi=1$.

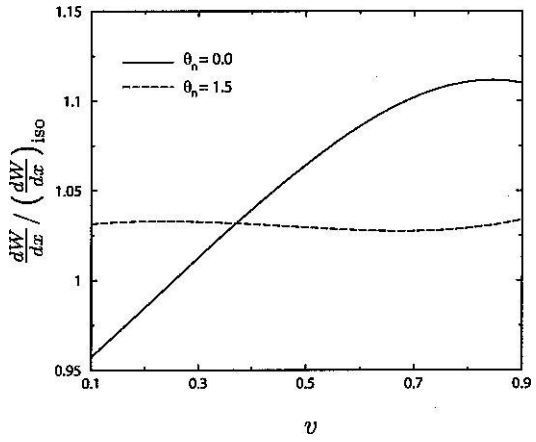

FIG. 18. Energy loss for angles $\theta_n=\{0,1.5\}$ as a function of v for $\xi=1$ and $e=0.3$.

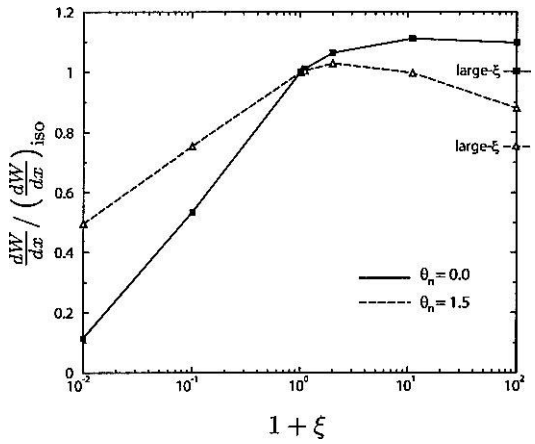

FIG. 19. Energy loss for angles $\theta_n=\{0,1.5\}$ as a function of ξ for $v=0.5$ and $e=0.3$. Lines on the right hand side of the plot frame indicate results obtained in the large-ξ limit.

As a side result we demonstrated that in the isotropic case the canonical result from Braaten and Thoma [12] has a correction which comes from the dependence of the result on the scale introduced to separate the soft and hard contributions to the energy loss. The residual dependence on the separation scale was then used to estimate the theoretical uncertainty of the resulting calculation for both the isotropic and anisotropic case.

Our final results indicate that for anisotropic QED plasmas there can be a significant directional dependence of the energy loss for highly relativistic fermions if there is a strong momentum-space anisotropy present in the electron distribution function. It should be mentioned that we have assumed here that the heavy fermion is infinitely massive. In the realistic case when the fermion mass is on the order of the muon mass the result obtained here should be reliable for velocities $0.6\lesssim v\lesssim 0.95$ [12].

We have concentrated here on the collisional energy loss in QED. In order to extend the result to QCD there will be a modification of the hard energy loss due to the fact that the fermion-boson scattering diagrams do not cancel against one another in this case. Besides this, the only modification required will be to adjust the Debye mass so that it corresponds to the QCD Debye mass. One complication will come from the fact that the quark and gluon distribution functions can, in general, have different momentum-space anisotropies; however, there should be an independent matching of logarithms coming from the quark and gluonic sectors. This work is currently in progress.

ACKNOWLEDGMENTS

M.S. and P.R. would like to thank A. Ipp, A. Rebhan, and M. Waibel for discussions. M.S. was supported by the Austrian Science Fund Project No. M689. P.R. was supported by the Austrian Science Fund Project No. P14632.

[1] PHENIX Collaboration, K. Adcox *et al.* Phys. Rev. Lett. **88**, 192303 (2002).
[2] PHENIX Collaboration, J.L. Nagle *et al.* Nucl. Phys. **A715**, 252 (2003).
[3] L.V. Gribov, E.M. Levin, and M.G. Ryskin, Phys. Rep. **100**, 1 (1983); A.H. Mueller and J.w. Qiu, Nucl. Phys. **B268**, 427 (1986); J.P. Blaizot and A.H. Mueller, *ibid.* **B289**, 847 (1987); L. McLerran and R. Venugopalan, Phys. Rev. D **49**, 2233 (1994); **49**, 3352 (1994); **50**, 2225 (1994); I. Balitskii, Nucl. Phys. **B463**, 99 (1996); J. Jalilian-Marian, A. Kovner, L. McLerran, and H. Weigert, Phys. Rev. D **55**, 5414 (1997); Yu.V. Kovchegov and A.H. Mueller, Nucl. Phys. **B529**, 451 (1998); Yu.V. Kovchegov, Phys. Rev. D **60**, 034008 (1999); **61**, 074018 (2000).
[4] R. Baier, A.H. Mueller, D. Schiff, and D.T. Son, Phys. Lett. B **502**, 51 (2001).
[5] E.S. Weibel, Phys. Rev. Lett. **2**, 83 (1959).
[6] S. Mrówczyński, Phys. Lett. B **314**, 118 (1993).
[7] S. Mrówczyński, Phys. Rev. C **49**, 2191 (1994).
[8] S. Mrówczyński, Phys. Lett. B **393**, 26 (1997).
[9] J. Randrup and S. Mrówczyński, Phys. Rev. C **68**, 034909 (2003).
[10] P. Romatschke and M. Strickland, Phys. Rev. D **68**, 036004 (2003).
[11] P. Arnold, J. Lenaghan, and G.D. Moore, J. High Energy Phys. **08**, 002 (2003).
[12] E. Braaten and M. Thoma, Phys. Rev. D **44**, 1298 (1991); **44**, R2625 (1991).
[13] J.D. Bjorken, Fermilab Report No. PUB-82/59-THY (1982).
[14] M.H. Thoma and M. Gyulassy, Nucl. Phys. **B351**, 491 (1991).
[15] S. Mrówczyński, Phys. Lett. B **269**, 383 (1991).
[16] G.D. Moore, QCD Kinetic Theory (Lecture), Quantum fields in and out of equilibrium, University of Bielefeld, 2003.